

Real-time experimental demonstration of low-cost VCSEL intensity-modulated 11.25Gb/s optical OFDM signal transmission over 25km PON systems

E. Hugues-Salas,* R.P. Giddings, X.Q. Jin, J. L. Wei, X. Zheng, Y. Hong, C. Shu and J.M. Tang

School of Electronic Engineering, Bangor University, Dean Street, Bangor, LL57 1UT, UK
*e.hugues-salas@bangor.ac.uk

Abstract: The feasibility of utilising low-cost, un-cooled vertical cavity surface-emitting lasers (VCSELs) as intensity modulators in real-time optical OFDM (OOFDM) transceivers is experimentally explored, for the first time, in terms of achievable signal bit rates, physical mechanisms limiting the transceiver performance and performance robustness. End-to-end real-time transmission of 11.25Gb/s 64-QAM-encoded OOFDM signals over simple intensity modulation and direct detection, 25km SSMF PON systems is experimentally demonstrated with a power penalty of 0.5dB. The low extinction ratio of the VCSEL intensity-modulated OOFDM signal is identified to be the dominant factor determining the maximum obtainable transmission performance. Experimental investigations indicate that, in addition to the enhanced transceiver performance, adaptive power loading can also significantly improve the system performance robustness to variations in VCSEL operating conditions. As a direct result, the aforementioned capacity versus reach performance is still retained over a wide VCSEL bias (driving) current (voltage) range of 4.5mA to 9mA (275mVpp to 320mVpp). This work is of great value as it demonstrates the possibility of future mass production of cost-effective OOFDM transceivers for PON applications.

©2011 Optical Society of America

OCIS codes: (060.0060) Fiber optics and optical communications; (060.4080) Modulation; (060.3510) Laser, fibre.

References and links

1. J. Armstrong, "OFDM for optical communications," *J. Lightwave Technol.* **27**(3), 189–204 (2009).
2. N. Cvijetic, D. Qian, and J. Hu, "100 Gb/s optical access based on optical orthogonal frequency-division multiplexing," *IEEE Commun. Mag.* **48**(7), 70–77 (2010).
3. G. Chang, A. Chowdhury, Z. Jia, H. Chien, M. Huang, J. Yu, and G. Ellinas, "Key technologies of WDM-PON for future converged optical broadband access networks," *J. Opt. Commun. Netw.* **1**(4), C35–C50 (2009).
4. R. P. Giddings, X. Q. Jin, E. Hugues-Salas, E. Giacomidis, J. L. Wei, and J. M. Tang, "Experimental demonstration of a record high 11.25Gb/s real-time optical OFDM transceiver supporting 25km SMF end-to-end transmission in simple IMDD systems," *Opt. Express* **18**(6), 5541–5555 (2010).
5. A. Schimpf, D. Bucci, and B. Cabon, "Optimum biasing of VCSEL diodes for all-optical up-conversion of OFDM signals," *J. Lightwave Technol.* **27**(16), 3484–3489 (2009).
6. E. Giacomidis, X. Q. Jin, A. Tsokanos, and J. M. Tang, "Statistical performance comparisons of optical OFDM adaptive loading algorithms in multimode fiber-based transmission systems," *IEEE Photon. J.* **2**, 1051–1059 (2010).
7. X. Zheng, X. Q. Jin, R. P. Giddings, J. L. Wei, E. Hugues-Salas, Y. H. Hong, and J. M. Tang, "Negative power penalties of optical OFDM signal transmissions in directly modulated DFB laser-based IMDD systems incorporating negative dispersion fibers," *IEEE Photon. J.* **2**(4), 532–542 (2010).
8. S. Lee, F. Breyer, S. Randel, D. Cárdenas, H. van den Boom, and A. Koonen, "Discrete multitone modulation for high-speed data transmission over multimode fibers using 850-nm VCSEL," *Optical Fiber Communication/National Fiber Optic Engineers Conference (OFC/NFOEC)*, (USA, 2009), Paper OWM2.

9. T. Duong, N. Genay, P. Chanclou, and B. Charbonnier, "10Gbit/s transmission over 2.5GHz bandwidth by direct modulation of commercial VCSEL and multi-mode FP lasers using adaptively modulated optical OFDM modulation for passive optical network", European Conference on Optical Communication (ECOC), (Brussels, 2008), paper We.1.F.4.
10. R. P. Giddings, E. Hugues-Salas, X. Q. Jin, J. L. Wei, and J. M. Tang, "Experimental demonstration of real-time optical OFDM transmission at 7.5 Gb/s over 25-km SSMF using a 1-GHz RSOA," *IEEE Photon. Technol. Lett.* **22**(11), 745–747 (2010).
11. R. P. Giddings, E. Hugues-Salas, B. Charbonnier, and J. M. Tang, "Experimental demonstration of real-time optical OFDM transmission at 11.25 Gb/s over 500m MMFs employing directly modulated DFB lasers," *IEEE Photon. Technol. Lett.* **23**(1), 51–53 (2011).
12. D. Qian, T. T. Kwok, N. Cvijetic, J. Hu, and T. Wang, "41.25 Gb/s real-time OFDM receiver for variable rate WDM-OFDMA-PON transmission", Optical Fiber Communication/National Fiber Optic Engineers Conference (OFC/NFOEC), (USA, 2010), Paper PDPD9.
13. R. P. Giddings, X. Q. Jin, and J. M. Tang, "First experimental demonstration of 6Gb/s real-time optical OFDM transceivers incorporating channel estimation and variable power loading," *Opt. Express* **17**(22), 19727–19738 (2009).
14. X. Q. Jin, R. P. Giddings, and J. M. Tang, "Real-time transmission of 3 Gb/s 16-QAM encoded optical OFDM signals over 75 km SMFs with negative power penalties," *Opt. Express* **17**(17), 14574–14585 (2009).
15. J. L. Wei, C. Sánchez, R. P. Giddings, E. Hugues-Salas, and J. M. Tang, "Significant improvements in optical power budgets of real-time optical OFDM PON systems," *Opt. Express* **18**(20), 20732–20745 (2010).
16. R. Dischler, A. Klekamp, F. Buchali, W. Idler, E. Lach, A. Schippel, M. Schneiders, S. Vorbeck, and R. Braun, "Transmission of 3x253-Gb/s OFDM-superchannels over 764 km field deployed single mode fibers", Optical Fiber Communication/National Fiber Optic Engineers Conference (OFC/NFOEC), (USA, 2010), Paper PDPD2.

1. Introduction

Optical orthogonal frequency division multiplexing (OOFDM) [1] has been considered as one of the strongest contenders for practical implementation in next-generation, high-speed passive optical networks (PONs) [2,3]. This is because OOFDM has a large number of inherent and unique advantages including, for example, potential for providing cost-effective technical solutions by fully exploiting the rapid advances in modern digital signal processing (DSP) technology, and considerable reduction in transmission system complexity owing to its great resistance to dispersion impairments and efficient utilization of channel spectral characteristics. Apart from the abovementioned advantages, OOFDM is also capable of offering, in both the frequency and time domains, hybrid dynamic allocation of broad bandwidth among various end-users [2].

In order for OOFDM PON systems to become sufficiently cost-effective for future mass deployment, the utilization of low-cost intensity modulators in OOFDM transceivers is crucial, as typical directly modulated DFB lasers (DMLs) employed in previously demonstrated end-to-end real-time OOFDM transceivers [4] take the majority of the transceiver cost. The use of vertical cavity surface-emitting lasers (VCSELs) as intensity modulators in real-time OOFDM transceivers is very promising, as they not only allow the desired transceiver cost target to be achieved, but also have salient advantages such as low power consumption, high reliability, long lifetime, as well as easy packaging and testing [5]. Moreover, the availability of multi-wavelength and multi-dimensional VCSEL arrays may further improve, in a cost-effective manner, the flexibility and scalability of wavelength division multiplexing (WDM) PONs. The significant disadvantage associated with a typical VCSEL intensity modulator is its low modulation bandwidth, which can, however, be efficiently utilized by further enhancing spectral efficiency through the use of adaptive modulation [6]. Furthermore, the performance limitations due to the frequency chirp and modulation nonlinearities associated with a directly modulated VCSEL in intensity modulation and direct detection (IMDD) PON systems can also be compensated, to some extent, by adaptive modulation [7].

The transmission performance of VCSEL intensity modulator-based IMDD OOFDM systems has been reported in [8,9]. However, both works were undertaken using off-line DSP approaches, which do not consider the limitations imposed by the precision and speed of practical DSP hardware for realizing end-to-end real-time transmission. Recently, by making use of various intensity modulators such as DMLs [4] and reflective semiconductor optical amplifiers (RSOAs) [10], we have experimentally demonstrated end-to-end real-time single

IFFT/FFT-based OOFDM transceivers at signal bit rates of up to 11.25Gb/s in 25km standard single-mode fibre (SSMF)-based PON systems and 500m multi-mode fibre (MMF) systems [11]. Recently, a 41.25 Gb/s real-time OOFDM receiver has also been experimentally demonstrated using multiple FFTs [12]. The work shows the feasibility of utilizing DSP hardware to support future high data rates.

The thrust of the present paper is to experimentally explore, for the first time, the feasibility of utilizing low-cost, un-cooled VCSEL intensity modulators in previously developed end-to-end real-time OOFDM transceivers at 11.25Gb/s [4,11] for cost-sensitive PON applications. In the present real-time OOFDM transceivers, on-line performance monitoring of total channel bit error rate (BER), individual subcarrier BER and system frequency response are also implemented. These on-line monitoring functions provide vital information for live control of digital signal power, signal clipping level, digital amplitude of individual subcarriers (here referred to as adaptive power loading) and VCSEL operating conditions to enable live maximization of system performance via minimizing the limitations set by low modulation bandwidths of cheap optical/electrical components.

Here it is worth mentioning that “adaptive power loading” means a live procedure of adaptive adjustment of digital amplitude of each individual subcarrier via the receiver information feedback to the transmitter to enable the OOFDM transceiver to effectively compensate for the system frequency response roll-off effect associated with a specific transmission system. The technique provides the OOFDM transceivers with great adaptability to variations in system frequency response, which maximizes the signal capacity versus reach performance and improves system flexibility and performance robustness, as discussed in Section 3.3. A sufficiently large system frequency response change, which necessitates the subcarrier power re-distribution from time to time, may occur due to the replacement of optical/electrical components, component aging, variation in operating conditions and system reconfigurations. As reported in [4], the minimum (maximum) loaded subcarrier power level is determined by the relative quantisation noise (dynamic power range of the IFFT/FFT). Finally, adaptive power loading utilizes the limited available power and just re-distributes the power among various subcarriers, thus it does not affect the overall power consumption of the OOFDM transceiver.

2. Real-time transceiver architecture and experimental system setup

The detailed end-to-end real-time experimental system setup is shown in Fig. 1. The VCSEL-based real-time OOFDM transceiver is implemented with field programmable gate arrays (FPGAs) for the high-speed DSP and a 4GS/s DAC/ADC. The IMDD PON system consists of a 25km SSMF without chromatic dispersion compensation. Table 1 presents a list of key parameters adopted in the experimental setup. It should be noted that the OOFDM transceiver architecture adopted here is very similar to those reported in [4,11,13], with real-time DSP being employed to perform functionalities such as IFFT/FFT algorithms, channel estimation, on-line performance monitoring and live parameter optimization. In comparison with the system setups reported in [4,11,13], the major differences in the current system are: (1) the use of a low-cost VCSEL for intensity modulation, (2) signal encoding in the transmitter and decoding in the receiver are performed using 32-QAM or 64-QAM. The use of these two signal modulation formats is to examine the highest achievable system performance and identify the dominant physical mechanisms limiting the maximum achievable transmission performance.

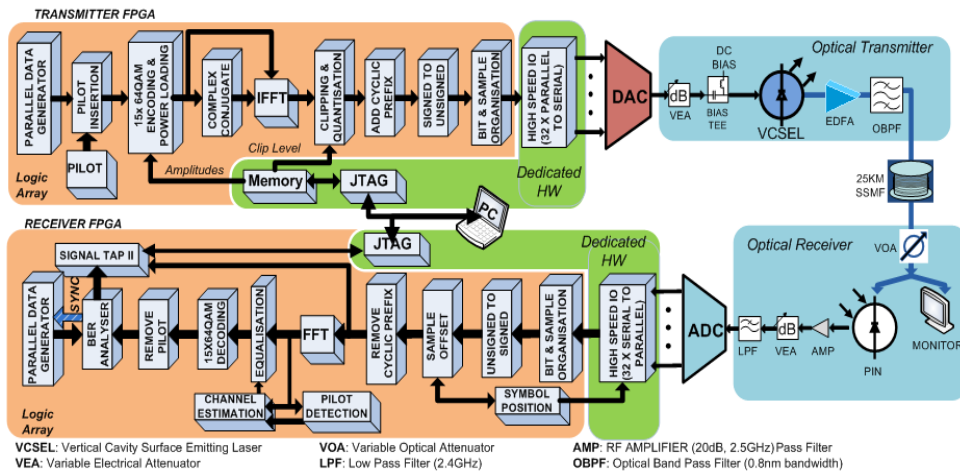


Fig. 1. End-to-end real-time FPGA-based OOFDM transceiver architectures and an IMDD 25km SSMF system using a directly modulated VCSEL.

In the transmitter FPGA, pseudo random data sequences generate a stream of 84-bit (70-bit) parallel words for 64-QAM (32-QAM) encoding. Based on the approach detailed in [14], each of these parallel words is combined with a fixed 6-bit (5-bit) pilot word for channel estimation. The combined 90-bit (75-bit) words are mapped onto 15 parallel 64-QAM (32-QAM) encoders. Considering the parameters listed in Table 1, for 64-QAM (32-QAM) signal modulation format, the OOFDM transmitter produces a raw signal bit rate of 11.25Gb/s (9.375Gb/s), of which 9Gb/s (7.5Gb/s) can be employed to carry user data, as a cyclic prefix length of 2ns per OOFDM symbol is adopted for all the transceiver designs. It should also be noted that the implemented channel estimation function only reduces the net signal bit rate by approximately 0.001% [14].

The real-valued, unsigned electrical OFDM signal emerging from the DAC output port is adjusted by a variable electrical attenuator to produce a driving signal with an amplitude of ~320mVpp. Simultaneously, via a bias tee an optimum DC bias current of 5.57mA is combined with the driving signal to directly modulate a fiber-tailed VCSEL operating at 1550nm. Under the above-mentioned VCSEL operating conditions, the output power of the VCSEL is -5.4dBm, which is boosted by an EDFA to fix the optical launch power at 7.8dBm.

In the receiver, a 12.38GHz, linear PIN detector directly detects the transmitted optical signal. The electrical output signal from the PIN is amplified to an optimum level to provide a suitable amplitude prior to digitization by an ADC. Similar to procedures reported in [4,10,11,13,14], only 15 data-carrying subcarriers are chosen for channel estimation and data recovery.

3. Experimental results

To identify optimum operating conditions of the VCSEL intensity modulators and simultaneously explore the maximum achievable transmission performance of the present PON system, in this paper, different system configurations are investigated, which are defined below:

- Case I. Analogue back-to-back. The DAC output in the transmitter is directly connected to the electrical attenuator input in the receiver.
- Case II. Optical back-to-back. The optical output of the band-pass filter in the transmitter is directly connected to the variable optical attenuator input in the receiver.
- Case III. An entire IMDD 25km SSMF PON system, as shown in Fig. 1.

Table 1. Transceiver and system parameters

Parameter	Modulation Format	
	64-QAM	32-QAM
		value
DAC & ADC sampling rate		4GS/s
DAC & ADC resolution		8 bits
Total number of IFFT/FFT points		32
Data-carrying subcarriers		15
n-th subcarrier frequency		$n \times 125\text{MHz}$
Symbol rate		100MHz
Modulation format on all subcarriers	64-QAM	32-QAM
Data bits per symbol	84 bits	70 bits
Pilot bits per symbol	6 bits	5 bits
Total bits per symbol	90 bits	75 bits
Error count period	88,500 symbols (7965000bits)	88,500 symbols (6637500bits)
Raw signal bit rate	11.25Gb/s	9.375Gb/s
Net signal bit rate	9Gb/s	7.5Gb/s
Cyclic prefix duration		2ns
Small-signal VCSEL modulation bandwidth		3.63GHz
Optimum VCSEL bias current		5.57mA
Optimum VCSEL driving voltage		320mVpp
VCSEL output power (optimum operating conditions)		-5.4dBm
VCSEL wavelength (optimum operating conditions)		1550nm
PIN detector bandwidth		12.38 GHz
PIN detector sensitivity		-19dBm ⁽¹⁾
SSMF dispersion parameter at 1550nm		18ps/(nm·km)

(1) Corresponding to 10^{-10} BER, PRBS $2^{31}-1$. NRZ @10Gb/s

3.1 System frequency responses

For the aforementioned various system configurations, the system frequency responses measured at individual subcarrier frequencies are plotted in Fig. 2. The measurements are performed from the input of the IFFT in the transmitter to the output of the FFT in the receiver and each measured system frequency response is normalised to its corresponding first subcarrier power. For Case I, a maximum 7.8dB system frequency response roll-off occurs, which is a direct result of the on-chip filtering in the DAC and its inherent $\sin(x)/x$ response [4]. Compared to Case I, Case II shows an extra 4dB system frequency response roll-off at high subcarrier frequencies. This is mainly attributed to nonlinearities of the VCSEL intensity modulator under the adopted operating conditions. In Case III, a maximum 12.5dB system frequency response roll-off is observed in the high subcarrier frequency region. The observed system frequency response difference between Case II and Case III is due to the IMDD nature of the transmission system and the VCSEL frequency chirp effect.

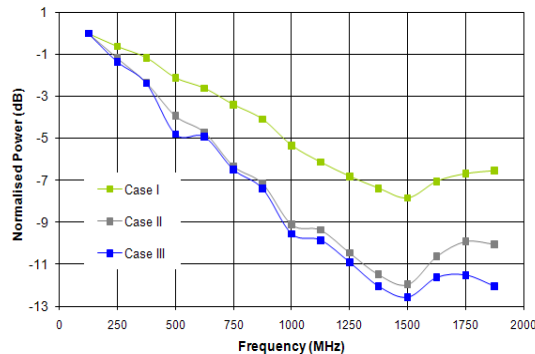


Fig. 2. System frequency responses of different system configurations: Case I. Analog back-to-back; Case II. Optical back-to-back and Case III. Entire IMDD 25km VCSEL-based SSMF system.

For Case III using 32-QAM and 64-QAM, based on the adaptive power loading procedure described in [4], the effectiveness of adaptive power loading in combating the system frequency response roll-off effect is examined in Fig. 3, where the loaded subcarrier power distributions in the transmitter are presented together with the received subcarrier power distributions in the receiver, all of which are normalized to the power of the corresponding first subcarrier. As expected, Fig. 3 indicates that adaptive power loading can efficiently compensate for the VCSEL-based IMDD OOFDM system frequency response roll-off effect. It should be pointed out that the differences of the loaded/received subcarrier powers between the 32-QAM and 64-QAM cases in Fig. 3 are due to the fact that a lower signal modulation format is more tolerant to the quantization effect at low signal amplitudes. This reduces the minimum allowed subcarrier amplitude, thus leading to an increased amplitude dynamic range.

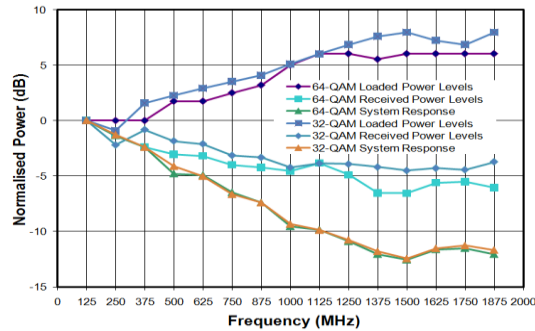


Fig. 3. Loaded/received subcarrier power levels and system frequency response for Case III using 32-QAM and 64-QAM.

To further verify the above statement, the 64-QAM-encoded OOFDM signal spectra at the output of the VCSEL intensity modulator with equal power loading and adaptive power loading are compared in Fig. 4. It can be seen in Fig. 4 that, for the case of utilizing equal power loading, a sharp decay of the OOFDM signal spectrum occurs. On the contrary, adaptive power loading gives rise to a relatively flat OOFDM signal spectrum.

Under the optimum loaded subcarrier power profiles presented in Fig. 3, the measured subcarrier error distributions are shown in Fig. 5 for Case III. It can be seen in Fig. 5 that adaptive power loading enables almost uniform subcarrier error distributions with a less than $\pm 12.5\%$ ($\pm 6\%$) variation for 64-QAM (32-QAM). This confirms, once again, that the adaptive power loading technique can effectively compensate for the system frequency response roll-off effect, thus resulting in an acceptable total channel BER obtained, as discussed in Subsection 3.2. The occurrence of the highest error peak corresponding to the 15th subcarrier in Fig. 5 is mainly due to the following two physical mechanisms: (1) the residual received power roll-off effect induced by the finite dynamic subcarrier power variation range, as shown in Fig. 3; (2) imperfect subcarrier orthogonality-induced inter-channel interference (ICI). Imperfect orthogonality between different subcarriers within a symbol arises due to the quasi-periodic structure of time domain OFDM symbols. Such an error peak can be considerably reduced when the signal extinction ratio of the OOFDM signal is increased [15].

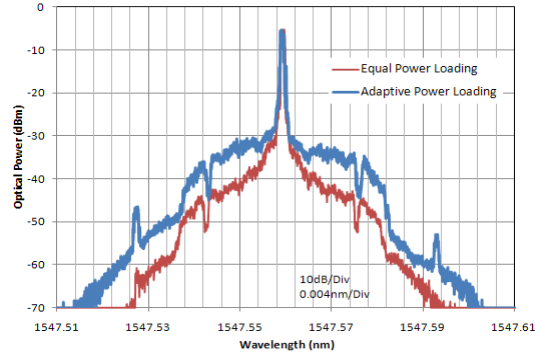


Fig. 4. Real-time 64-QAM-encoded OOFDM signal spectra at the output of the VCSEL intensity modulator with equal power loading and adaptive power loading.

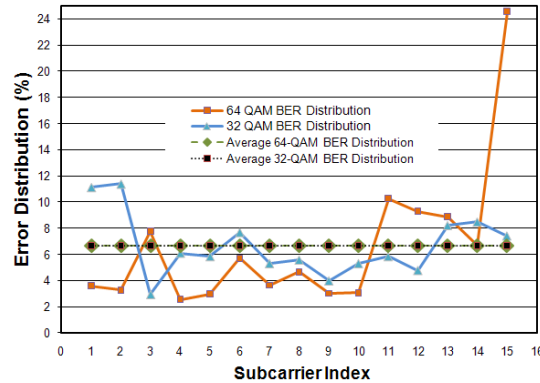


Fig. 5. Typical subcarrier error distribution for 32-QAM and 64-QAM over 25km SSMF when adaptive power loading is used.

3.2 Total channel BER performance

Based on the optimum loaded subcarrier power profiles, end-to-end real-time transmission of 11.25Gb/s (9.375Gb/s) 64-QAM- (32-QAM)-encoded OOFDM signals is experimentally demonstrated over 25km SSMF IMDD PON systems involving VCSEL intensity modulators. Figure 6 shows the measured total channel BER performance for both Case II and Case III.

From Fig. 6, it is observed that, for 11.25Gb/s 64-QAM-encoded OOFDM signals, the total channel BERs of 1.1×10^{-3} and 1.2×10^{-3} are obtainable for Case II and Case III, respectively. The corresponding power penalty at a FEC limit of 4×10^{-3} [16] is approximately 0.5dB. Whilst for 9.375Gb/s 32-QAM-encoded OOFDM signals, the total channel BERs as low as 5.2×10^{-5} and 6.9×10^{-5} are feasible for Case II and Case III, respectively, with a negligible power penalty at the above-mentioned FEC limit. Such substantial improvement in system BER performance for a lower signal modulation format indicates that the dynamic system frequency response roll-off effect does not considerably affect the system performance due to the use of adaptive power loading. The main physical factor determining the minimum achievable BER is the relatively low extinction ratio of the VCSEL intensity-modulated OOFDM signal [15]. Generally speaking, a small signal extinction ratio reduces the effective signal-to-noise ratio (SNR) of a received OOFDM signal for a specific photon detector. Therefore, an OOFDM signal encoded using a high signal modulation format is more susceptible to the effective SNR reduction, compared to an OOFDM signal encoded using a low signal modulation format. This is the physical mechanism underpinning the BER difference between the 64-QAM and 32-QAM cases, as shown in Fig. 6. In addition, the error-floor like BER performance observed in Fig. 6 is a

result of the low signal extinction ratio-induced small effective SNR of the received OOFDM signal.

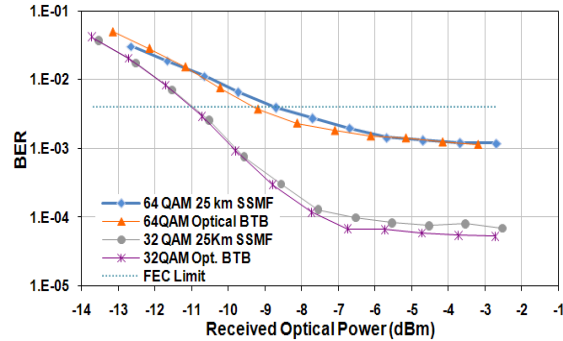


Fig. 6. BER performance for optical back-to-back and transmission over 25km SSMFs for 32-QAM and 64-QAM modulation formats.

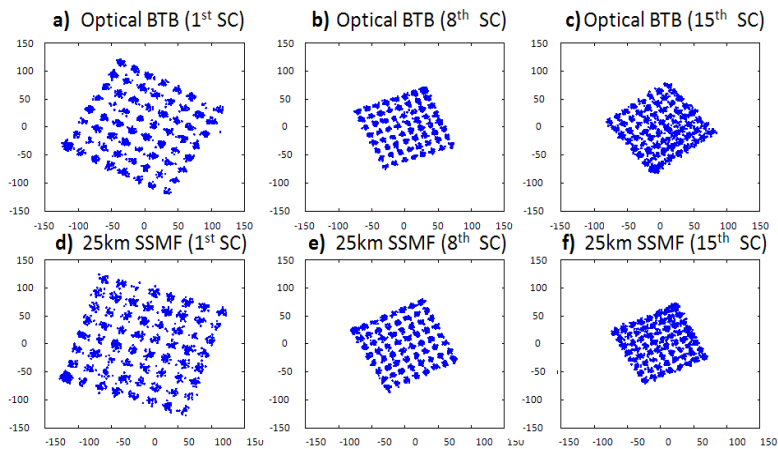


Fig. 7. Received 64-QAM constellations of individual subcarriers before equalization. Optical back-to-back, total channel BER = 1.1×10^{-3} (a, b, c) 25km SSMF, total channel BER = 1.2×10^{-3} , (d, e, f).

Representative constellations of individual subcarriers of the 11.25Gb/s 64-QAM-(9.375Gb/s 32-QAM)-encoded OOFDM signals corresponding to the total channel BERs of 1.1×10^{-3} for Case II and 1.2×10^{-3} for Case III (5.2×10^{-5} for Case II and 6.9×10^{-5} for Case III) are presented in Fig. 7 (Fig. 8). These constellations are recorded prior to performing channel equalization in the receiver. All the constellations show a variation in amplitude level corresponding to the power variation shown in Fig. 3. In comparison with their optical back-to-back counterparts, the constellations for Case III show very little deviations. This is reflected in the small BER difference between these two cases, as shown in Fig. 6.

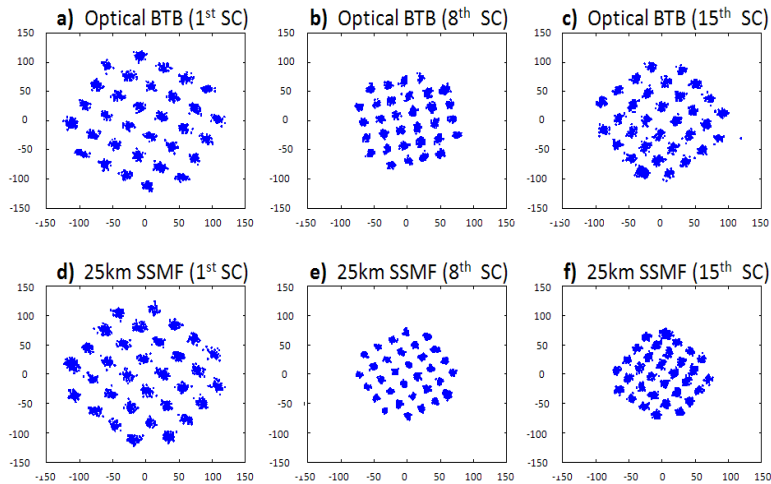


Fig. 8. Received 32-QAM constellations of individual subcarriers before equalization. Optical back-to-back, total channel BER = 5.2×10^{-5} (a, b, c) 25km SSMF, total channel BER = 6.9×10^{-5} (d, e, f).

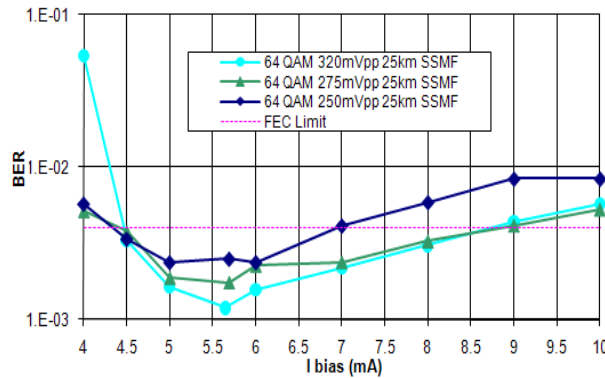


Fig. 9. Bias and driving current dependent total channel BER performance.

3.3 System performance robustness

As a large dynamic operating condition range of the adopted intensity modulator can significantly improve the system performance robustness, from the practical system design point of view, it is greatly advantageous if the VCSEL intensity modulator can operate over a wide range of DC bias currents and driving voltages, without considerably compromising the system performance compared to that obtained under the identified optimum intensity modulator operating conditions. In this subsection, we show experimentally that, apart from the considerable improvement in transmission performance, adaptive power loading can also significantly extend the VCSEL dynamic operating condition range, due to its capability of compensating for the dependence of the system frequency response upon variations in DC bias current and driving voltage.

Figure 9 shows the total channel BER performance as a function of DC bias current and driving voltage for Case III using 64-QAM. In obtaining this figure, the DC bias current varies in a range of 4mA to 10mA, as the VCSEL's lasing threshold is 2mA and the absolute maximum forward current specified by the manufacturer is 15mA. In addition, the applied driving voltage also varies within a large range of 250mVpp to 320mVpp. In the experimental measurements, live adjustment of the loaded subcarrier power profiles is performed for each

of the selected DC bias currents and/or driving voltages. It should also be noted, in particular, that no VCSEL dynamic operating range exists for equal power loading, as equal power loading does not enable the present transmission system to operate under the FEC limit even when the identified optimum VCSEL operating conditions are adopted.

It is very interesting to note in Fig. 9 that total channel BERs below the FEC limit are obtainable for bias currents ranging from 4.5mA to 9mA and driving voltages ranging from 275mVpp to 320mVpp. A 2mA reduction of the aforementioned bias current range, i.e., from 9mA to 7mA, decreases the minimum allowed driving voltage to a value as low as 250mVpp, thus broadening the driving voltage range by 25mVpp. For DC bias currents of less than the optimum value of 5.57mA, the BER reduction with increasing bias current is mainly due to the reduced signal clipping effect, because a smaller portion of the lower part of the driving signal penetrates into the region below the VCSEL lasing threshold. On the other hand, for DC bias currents of higher than the optimum value of 5.57mA, the BER increase with increasing bias current is mainly due to the large DC component-induced reduction in signal extinction ratio: a low signal extinction ratio increases OOFDM signal susceptibility to noise [15]. Moreover, Fig. 9 also shows that, for a given bias current, an increase in driving voltage decreases the total channel BER over almost the entire bias current and driving voltage regions. This suggests, once again, that, in comparison with the VCSEL frequency chirp effect, a low extinction ratio of the VCSEL intensity-modulated OOFDM signal is a dominant factor limiting the performance of the current transmission system.

4. Conclusions

The feasibility of utilising low-cost, un-cooled VCSELs as intensity modulators in previously demonstrated real-time OOFDM transceivers has been extensively explored experimentally, for the first time, in terms of achievable signal bit rates, physical mechanisms limiting the transceiver performance and performance robustness. Making use of such transceivers, end-to-end real-time transmission of 11.25Gb/s 64-QAM-encoded OOFDM signals over 25km SSMF IMDD PON systems has been experimentally demonstrated with a power penalty of 0.5dB. It has been identified that a low extinction ratio of the VCSEL intensity-modulated OOFDM signal is the dominant factor determining the maximum obtainable system performance. Experimental investigations have also indicated that, in addition to the enhanced transceiver performance, adaptive power loading can significantly improve the system performance robustness to variations in VCSEL operating conditions. As a direct result, the aforementioned capacity versus reach performance is still retained over a wide VCSEL bias current (driving voltage) range of 4.5mA to 9mA (275mVpp to 320mVpp). Given the fact that conventional DFB lasers take the majority of the OOFDM transceiver cost, this work is of great value as it demonstrates the possibility of future mass production of cost-effective OOFDM transceivers for PON applications. In addition, the utilisation of large modulation bandwidth (>10GHz) and highly linear VCSELs with steep L-I curves in the OOFDM systems could increase the VCSEL-based OOFDM transceiver speeds to 40Gb/s. Such VCSELs are becoming commercially available and have the potential for achieving low cost when mass produced.

Acknowledgements

This work was partly supported by the EC's Seventh Framework Programme (FP7/2007-2013) within the project ICT ALPHA under grant agreement n° 212 352, and in part by the Welsh Assembly Government and The European Regional Development fund. The authors would also like to thank APEX technologies for the loan of the optical spectral analyser (AP2440A).